# Transition-metal-doped ZnO Nanowire Arrays Embedded in Anodic Alumina Membrane by a Sol Precipitation Method

Ming Wang,* Xueli Cao, Huixin Wang, Guomin Hua, Yongxing Lin, and Lide Zhang
*Key Laboratory of Materials Physics, Institute of Solid State Physics, Chinese Academy of Science,*
*Hefei, Anhui 230031, P. R. China*

(Received July 4, 2006; CL-060758; E-mail: mwang@issp.ac.cn)

We report the synthesis of transition-metal ($Co^{2+}$)-doped ZnO nanowire arrays embedded in anodic alumina membrane (AAM) by a sol precipitation method. The direct synthetic method ensures the successful doping of cobalt in the ZnO nanocrystals and exhibiting bivalent state.

Doping of transition metal into semiconductor materials to obtain ferromagnetism, which is called dilute magnetic semiconductors (DMSs), has attracted intensive interests in the spintronics research fields.[1,2] Since the physicists predicted that transition-metal-doped ZnO should be favorable candidate for room-temperature ferromagnetism,[3] many reports on the room-temperature ferromagnetism of doped ZnO have been published.[4–6] Recently, the ferromagnetism was presented by Gamelin group using a direct synthetic method in which doped ZnO colloids were used as precursors for spin coating films.[7,8] This result also shows that the direct chemical synthesis based on soft chemical strategy is an effective method for doping of nanocrystals.

In the past few years, the AAM-based synthesis method has been proved to be an effective route for fabricating one-dimensional nanostructured metals and semiconductors.[9,10] Fabrication of various oxide nanowire/nanotube arrays in AAM via a sol–gel method has been reported recently.[11,12] In this letter, we reported on the fabrication of $Co^{2+}$-doped ZnO nanowire arrays by precipitation of nanocrystals in AAM in the sol solution for the first time. Because many doped colloidal oxide nanocrystals such as $TiO_2$, $SnO_2$ can be synthesized from the direct synthetic method,[13,14] we believe that the method presented in this letter can be extended to fabricate many other oxide nanostructures for applications of spintronics devices. The synthesis route also allows for the doping of different transition metal (Mn, Ni, Fe), but this report is limited to the cobalt-doped ZnO nanowires.

The fabrication of the sample includes two steps: synthesis of doped colloidal ZnO nanocrystals and subsequent precipitation of these nanocrystals in AAM template. In a typical fabrication, 0.06 g of $LiOH \cdot H_2O$ and 0.22 g of $Zn(OAc)_2 \cdot 2H_2O$ were dissolved in 30 and 70 mL of ethanol respectively, and then the lithium hydroxide was added by dropwise into the zinc acetate solution under constant stirring. Transition metal was introduced by addition of desired amount of $Co(OAc)_2 \cdot 4H_2O$ to the $Zn(OAc)_2 \cdot 2H_2O$ precursor solution. Nanocrystals were precipitated by addition of heptane, washed with ethyl acetate, and resuspended in ethanol. The AAM with pore size of 60–80 nm, prepared using a two-step anodic anodization process as previously reported,[15] was inserted in the colloidal solution. The solution was placed in a dry oven at 80 °C for several hours. The sample was washed with deionized water and dried before characterisation. The absorption spectrum of the colloidal nanocrystals was collected using a Cary 5E. The fabricated nanowire arrays were characterized by means of X-ray powder diffractometer (Philips X'Pert Pro), field emission scanning electron microscopy (FE-SEM, FEI, Sirion 200), transmission electron microscopy (TEM, JEOL JEM-210CX). The composition was determined by energy dispersive X-ray spectroscopy (EDX, Inca Oxford, attached to the FE-SEM). The X-ray photoelectron spectrum (XPS) was collected on an ESCALAB MK X-ray photoelectron spectrometer.

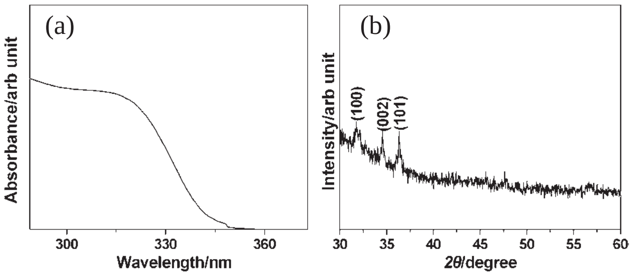

**Figure 1.** (a) Absorption spectrum of the as-prepared doped colloidal ZnO nanocrystals, (b) XRD pattern of the doped ZnO nanowire arrays in AAM.

As shown in Figure 1a, a significant blue shift of the band-edge absorption with respect to the bulk material (373 nm) was observed. This blue shift can be ascribed to the quantum-confined size effect. The size of these nanocrystals was estimated about 7 nm from the spectrum.[16] Figure 1b shows the XRD pattern of the sample. The peaks can be indexed to the wurtzite ZnO according to the standard JCPDS (No. 36-1451). Besides the peaks of ZnO, no other peak was detected, which indicates the successful doping of $Co^{2+}$ into ZnO structures without segregation of cobalt compounds.

The broadening of the ZnO peaks can be ascribed to the reduced grain size of the nanocrystals. The broad peak at the small angle comes from the amorphous phase of AAM.

Figure 2 shows the FE-SEM image of the obtained nanowire arrays. Before observation, the sample was etched in a 0.5 M NaOH solution. It can be observed that a large bundle of nanowires is roughly parallel to each other, and the diameters of these nanowires are about 60–80 nm, corresponding to the pore size of the AAM template. The length of the nanowires can extend to several micrometers, which depends on the AAM synthesis conditions. The nanowires are formed through high-dense stacking of small ZnO nanocrystals. The particles cleaveing to the nanowire surface are the ZnO particles aggregated in the colloidal solution and which can be removed easily by ultrasonic agitation (see TEM image of Figure 3a).

Figure 3a shows the TEM image of a single nanowire. The AAM was completely removed by etching of the sample in the 0.5 M NaOH solution and the nanowire arrays were dispersed

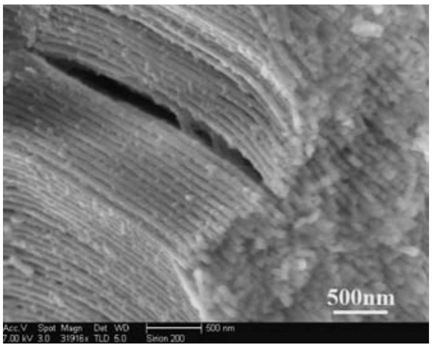

**Figure 2.** FE-SEM image of the doped ZnO nanowire arrays.

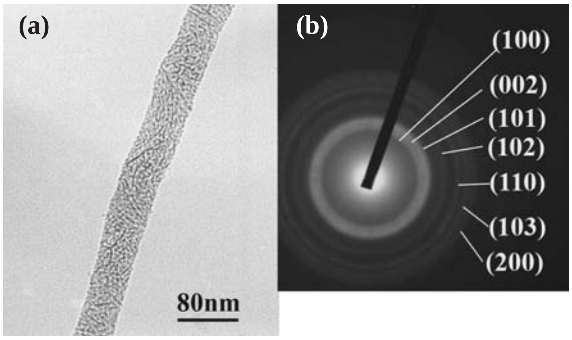

**Figure 3.** (a) TEM image of a single nanowire, (b) Its corresponding selected area electron diffraction (SAED) pattern.

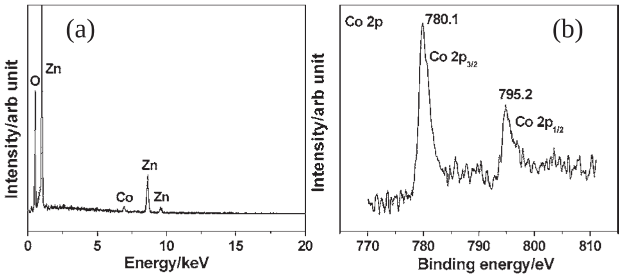

**Figure 4.** (a) Energy dispersive X-ray spectroscopy (EDX) of the $Co^{2+}$-doped ZnO nanowire arrays, (b) XPS spectrum of the Co 2p.

in ethanol by ultrasonic. It can be seen that the nanowire is constituted from a large amount of small spherical nanoparticles. The diameter of the nanowire is 60 nm. The nanowire has smooth surface, which indicates the nanowire was formed by compact stacking of the small ZnO nanocrystals. Its SAED pattern (Figure 3b) shows the polycrystalline character of the doped ZnO nanowires without other second phase.

The composition of the doped ZnO nanowires, determined by energy dispersive X-ray spectroscopy, was shown in Figure 4a. The peak at 0.53 keV can be ascribed to oxygen and the peaks at 1.01, 8.63, 9.58 keV can be ascribed to zinc. The signal at 6.94 keV can be assigned to cobalt. Figure 4b shows the X-ray photoelectron spectrum of the cobalt 2p. The $2p_{3/2}$ peak at 780.1 eV and the $2p_{1/2}$ peak at 795.2 eV can be assigned to $Co^{2+}$ coordinated to oxygen atoms.[17,18] This result indicates that this low-temperature method can avoid the emergence of second phase of Co or $Co_2O_3$.[19] The concentrations from the EDX and XPS are about 0.7 and 0.9 atom %, respectively, for the nominal 2 atom % doping sample. This result shows that only part of cobalt was doped into the ZnO structures and the other was washed during the synthetic process.

In summary, we have fabricated $Co^{2+}$-doped ZnO nanowire arrays by precipitation of doped colloidal nanocrystals in the AAM channels. This method is expected for fabrication of other doped oxide semiconductor nanostructures via a simple route, which has a significant importance in the spintronics research fields.

This work was supported by National Major Fundamental Project of China: Nanomaterials and Nanostructures (Grant No. 2005CB623603).

## References

1 H. Ohno, D. Chiba, F. Matsukura, T. Omiya, E. Abe, T. Dietl, Y. Ohno, K. Ohtani, *Nature* **2000**, *408*, 944.
2 S. A. Wolf, D. D. Awschalom, R. A. Buhrman, J. M. Daughton, S. von Molnár, M. L. Roukes, A. Y. Chthelkanova, D. M. Treger, *Science* **2001**, *294*, 1488.
3 T. Dietl, H. Ohno, F. Matsukura, J. Cibert, D. Ferrand, *Science* **2000**, *287*, 1019.
4 P. Sharma, A. Gupta, K. V. Rao, F. J. Owens, R. Sharma, R. Ahuja, J. M. O. Guillen, B. Johansson, G. A. Gehring, *Nat. Mater.* **2003**, *2*, 673.
5 D. P. Norton, S. J. Pearton, A. F. Hebard, N. Theodoropoulou, L. A. Boatner, R. G. Wilson, *Appl. Phys. Lett.* **2003**, *82*, 239.
6 K. R. Kittilstved, N. S. Norberg, D. R. Gamelin, *Phys. Rev. Lett.* **2005**, *94*, 147209.
7 N. S. Norberg, K. R. Kittilstved, J. E. Amonette, R. K. Kukkadapu, D. A. Schwartz, D. R. Gamelin, *J. Am. Chem. Soc.* **2004**, *126*, 9387.
8 K. R. Kittilstved, D. R. Gamelin, *J. Am. Chem. Soc.* **2005**, *127*, 5292.
9 L. Li, Y. Xiao, Y. Yang, G. Li, Y. Li, L. Zhang, *Chem. Lett.* **2005**, *34*, 1274.
10 Y. Li, G. W. Meng, L. D. Zhang, F. Phillipp, *Appl. Phys. Lett.* **2000**, *76*, 2011.
11 B. B. Lakshmi, P. K. Dorhout, C. R. Martin, *Chem. Mater.* **1997**, *9*, 857.
12 G. Wu, L. Zhang, B. Cheng, T. Xie, X. Yuan, *J. Am. Chem. Soc.* **2004**, *126*, 5976.
13 P. I. Archer, P. V. Radovanovic, S. M. Heald, D. R. Gamelin, *J. Am. Chem. Soc.* **2005**, *127*, 14479.
14 J. D. Bryan, S. A. Santangelo, S. C. Keveren, D. R. Gamelin, *J. Am. Chem. Soc.* **2005**, *127*, 15568.
15 H. Masuda, K. Fukuda, *Science* **1995**, *268*, 1466.
16 N. S. Pesika, Z. Hu, K. J. Stebe, P. C. Searson, *J. Phys. Chem. B* **2002**, *106*, 6985.
17 R. Dedryvére, S. Laruelle, S. Grugeon, P. Poizot, D. Gonbeau, J. M. Tarascon, *Chem. Mater.* **2004**, *16*, 1056.
18 J.-C. Dupin, D. Gonbeau, P. Vinatier, A. Levasseur, *Phys. Chem. Chem. Phys.* **2000**, *2*, 1319.
19 L. Yan, C. K. Ong, X. S. Rao, *J. Appl. Phys.* **2004**, *96*, 508.

Published on the web (Advance View) September 30, 2006; doi:10.1246/cl.2006.1234